Investigation of the short-time photodissociation dynamics of *trans*-1-bromo-2-iodoethane in the *A*-band absorption

Xuming Zheng and David Lee Phillips[a)]
Department of Chemistry, University of Hong Kong, Pokfulam Road, Hong Kong

(Received 29 June 1998; accepted 16 October 1998)

We have obtained resonance Raman spectra and absolute Raman cross section measurements at five excitation wavelengths within the *A*-band absorption for 1-bromo-2-iodoethane in cyclohexane solution. The resonance Raman spectra have most of their intensity in the fundamentals, overtones, and combination bands of six Franck–Condon active vibrational modes; the nominal CCI bend, C–I stretch, C–Br stretch, C–C stretch, CH_2 wag with the Br atom attached to the CH_2 group, and CH_2 wag with the I atom attached to the CH_2 group. The resonance Raman intensities and *A*-band absorption spectrum were simulated using a simple model and time-dependent wave packet calculations. The simulation results and normal mode descriptions were used to find the short-time photodissociation dynamics in terms of internal coordinate displacements. The *A*-band short-time photodissociation dynamics for *trans*-1-bromo-2-iodoethane show that the C–I, C–Br, and C–C bonds as well as the CCI, CCBr, HCC, ICH, and BrCH angles have significant changes during the initial stages of the photodissociation reaction. This indicates the photodissociation reaction has a large degree of multidimensional character and suggests that the bromoethyl photofragment receives substantial internal excitation in so far as the short-time photodissociation dynamics determines the energy partitioning. Comparison of our results for 1-bromo-2-iodoethane with the *A*-band short-time dynamics of iodoethane, 1-chloro-2-iodoethane, and 1,2-diiodoethane and the trends observed for their *A*-band absorption spectra suggest that both the C–I and C–Br bonds experience a noticeable amount of photoexcitation. © *1999 American Institute of Physics.* [S0021-9606(99)01503-2]

I. INTRODUCTION

The *A*-band photodissociation of iodoalkanes have been extensively studied as examples of direct photodissociation reactions and have played an important role in better understanding photodissociation dynamics and energy partitioning. The *A*-band absorption spectra of gas and solution phase iodoalkanes are unstructured and composed of three transitions ($^3Q_0$, $^1Q_1$, and $^3Q_1$).[1–3] The $^3Q_0$ transition gives rise to most of the oscillator strength of the *A*-band absorption and correlates with I* photofragments. Ground electronic state iodine atoms (I) can be formed in significant numbers from an electronic nonadiabatic curve crossing of the $^3Q_0$ state by the $^1Q_1$ state.[4–11] Molecular beam experiments measuring photofragment anisotropies have shown that the C–I bond cleavage associated with the *A*-band absorption of iodoalkanes takes place much quicker than the rotational period of the parent iodoalkane molecule.[11–18]

Iodomethane has been the most investigated iodoalkane molecule for the *A*-band photodissociation reaction. Magnetic circular dichroism (MCD) experiments found that the $^3Q_0$ transition near the center of the absorption band accounts for about 70%–80% of the oscillator strength and the $^3Q_1$ and $^1Q_1$ near the red and blue edges of the absorption band have the remaining oscillator strength.[2] High resolution time-of-flight photofragment spectroscopy experiments indicated some internal energy appears in the umbrella mode vibration of the methyl radical photofragment.[12,13] The vibrational and rotational state distributions of the methyl radical photofragment have been measured by multiphoton ionization (MPI),[19–21] coherent anti-Stokes Raman scattering (CARS),[22] diode laser absorption,[23] and other experiments.[24] Femtosecond time-resolved pump–probe experiments found that the iodomethane *A*-band photodissociation reaction occurred in less than 100 fs.[25,26] Resonance Raman spectroscopy was used to examine the short-time photodissociation dynamics. The resonance Raman spectra displayed long overtone progressions in the nominal C–I stretch vibrational mode and a smaller combination band progression in the nominal CH_3 umbrella mode fundamental plus C–I stretch overtones.[27–36] The contributions from electronic states other than $^3Q_0$ (e.g., $^3Q_1$ and $^1Q_1$) and possible effects of the $^3Q_0$ and $^1Q_1$ nonadiabatic curve crossing on the resonance Raman spectra were investigated using depolarization ratio measurements.[29,30,34] Solvation and solvent effects on the resonance Raman spectra and associated short-time photodissociation dynamics were also examined.[31–33] Different theoretical models and potential energy surfaces with varying degrees of sophistication have been used to elucidate the *A*-band photodissociation of iodoalkanes.[37–46] Fully quantum mechanical simulations using reasonably accurate *ab initio* potential energy surfaces were used to model much of the available experimental data for iodomethane and it seems that the major aspects of the *A*-band photodissociation of iodomethane have been elucidated.[45,46]

The *A*-band photodissociation reactions of larger iodoalkanes and dihaloalkanes have not been examined as compre-

a)Author to whom correspondence should be addressed.

hensively as iodomethane. However, studies carried out on other iodoalkanes (and dihaloalkanes) enable examination of how the molecular structure and substituents modify the photodissociation dynamics, energy partitioning to the photofragments and the probability of $^3Q_0$ to $^1Q_1$ curve crossing. Time-of-flight translational spectroscopy experiments for several different iodoalkanes indicate that as the alkyl group gets larger and/or more branched in structure then the degree of internal excitation of the alkyl radical photofragment increases.[11–18,47–55] Experimental measurements of the I*/I ratio a function of the structure and mass of parent iodoalkane found that more I photofragment is produced as the iodoalkane molecule increases in mass or becomes more branched in structure.[4–11,56–63] This suggests that the $^3Q_0$ to $^1Q_1$ curve crossing probability has some dependence on the degree of internal energy deposited into the alkyl photofragment; less of the available energy of the photodissociation is deposited into translation of the two photofragments as more of the available energy goes into internal excitation of the alkyl photofragment which leads to an increased curve crossing probability.

Two simple models for the photodissociation dynamics of direct bond cleavage reactions have been used to explain the energy partitioning of the *A*-band iodoalkane photodissociation reaction.[12,15–17] The ''rigid radical'' model makes the assumption that the alkyl radical maintains the same structure during the photodisscociation reaction and this leads to only internal excitation of the rotational degree of freedom of the alkyl radical.[12,15–17] On the other hand, the ''soft radical'' model can give rise to internal excitation of both the vibrational and rotational degrees of freedom of the alkyl radical. The ''soft radical'' model makes the assumption that the α-carbon atom is very weakly connected to the rest of the alkyl radical so that the C–I bond breaking leads to the α-carbon atom being pushed into the rest of the alkyl radical.[12,15–17] The energy disposal of most iodoalkanes seem to be nearer that given by the ''soft radical'' model than the values given by the ''rigid radical'' model.[12,15–17]

The ''rigid radical'' and ''soft radical'' models are close to two limits to how the α-carbon atom is bonded to the rest of the alkyl radical during the photodissociation. The ''rigid radical'' model α-carbon has far too strong bonding to the rest of the alkyl radical in order to maintain a rigid alkyl radical structure during the photodissociation and the ''soft radical'' model α-carbon has too weak bonding to the rest of the alkyl radical during the photodissociation. Both the ''rigid radical'' and ''soft radical'' models of the photodissociation dynamics do not realistically account for the α-carbon atom bonding to the rest of the alkyl radical during the photodissociation and more accurate models need to be developed for direct photodissociation dynamics and energy partitioning. Resonance Raman spectroscopy has been used to investigate the short-time photodissociation dynamics of several dihaloalkanes and higher iodoalkanes.[36,64–79] These studies showed that as the mass increases and/or the structure becomes more branched, then the intensity in nominal non-C–I stretch combination bands with the C–I stretch overtones increases relative to the C–I stretch overtone progression intensity. This trend may arise from more mixing of the internal coordinate motions in the normal coordinate descriptions of the Franck–Condon active modes and/or actual changes in the photodissociation dynamics. The short-time photodissociation dynamics of several higher iodoalkanes and dihaloalkanes have been determined using the results of normal coordinate calculations and resonance Raman intensity analysis.[67,72–79] These studies showed that the C–I bond cleavage takes place on a time-scale similar to the vibrational motions in the rest of the iodoalkane molecule and the Franck–Condon region dynamics seemed to be somewhere between the ''soft radical'' and ''rigid radical'' descriptions of the photodissociation dynamics.

We have obtained a partial *A*-band resonance Raman excitation profile and absolute Raman cross section measurements for 1-bromo-2-iodoethane in cyclohexane solution. Time-dependent wave packet calculations were done to simulate the experimental absorption spectrum and resonance Raman intensities in order to characterize the Franck–Condon region of the excited electronic state. The results of normal coordinate calculations were used in conjunction with the results of the resonance Raman intensity analysis to find the short-time photodissociation dynamics in easy to visualize internal coordinate changes. We compare our results for 1-bromo-2-iodoethane with those found previously for iodoethane, 1-chloro-2-iodoethane and 1,2-diiodoethane in order to investigate the effect of substitution of a hydrogen atom on the β-carbon atom by a more massive halogen atom. We also examine how the C–I bond breaking in the Franck–Condon region is influenced by the presence of an additional carbon–halogen chromophore.

II. EXPERIMENT

Spectroscopic grade cyclohexane solvent (Aldrich Chemical Company) and 1-bromo-2-iodoethane (99% from Strem custom synthesis) were used to prepare samples for the resonance Raman spectroscopy experiments. Resonance Raman spectra were obtained for 1-bromo-2-iodoethane in cyclohexane sample solutions with concentrations ranging from 0.4 M to 0.5 M. We have previously described the experimental apparatus and methods used to acquire the resonance Raman spectra and the reader is referred to these references for details.[69–75,77–79] The excitation laser for the resonance Raman experiments used $\sim$100 μJ loosely focused to a 1 mm diam on the flowing liquid sample. The methods detailed in Ref. 80 were used to correct the spectra for the reabsorption of the Raman scattered light by the sample solution and an intensity calibrated deuterium lamp were used to correct the resonance Raman spectra for the sensitivity of the whole collection system as a function of wavelength. The absolute resonance Raman cross sections of 1-bromo-2-iodoethane in cyclohexane solution were obtained relative to the absolute Raman cross section of the 802 cm^{-1} Raman band of cyclohexane solvent.[81,82]

III. CALCULATIONS

We have used a relatively simple model and time-dependent wave packet calculations[83–87] to simulate the resonance Raman intensities and *A*-band absorption spectrum of

1-bromo-2-iodoethane in cyclohexane solution so as to examine the major features of the short-time photodissociation dynamics. The model and computational results given here are not meant to be a comprehensive characterization of the resonance Raman and absorption spectra, but serve to give a modest start to better elucidate the vibrational mode-specific dynamics of the initial C–I bond breaking in 1-bromo-2-iodoethane. The modeling results shown here will also serve as a useful reference to which more thorough simulations can be compared to assess the significance of effects like the coordinate dependence of the transition dipole moment, anharmonicity, possible Duschinsky rotation of normal coordinates, and others.

The *A*-band absorption spectrum of 1-bromo-2-iodoethane was simulated using the following formula:

$$\sigma_A(E_L)=(4\pi e^2E_LM^2/3n\hbar^2c)\times\Sigma_iP_i\ \mathrm{Re}\left[\int_0^\infty\langle i|i(t)\rangle\exp[i(E_L+\epsilon_i)t/\hbar]\times\exp[-g(t)]dt\right]. \quad (1)$$

The resonance Raman cross sections were calculated from this formula,

$$\sigma_{R,}(E_L,\omega_s)=\Sigma_i\Sigma_fP_i\sigma_{R,i\to f}(E_L)\,\delta(E_L+\epsilon_i-E_s-\epsilon_f)$$

with

$$\sigma_{R,i\to f}(E_L)=(8\pi e^4E_S^3E_LM^4/9\hbar^6c^4)\left|\int_0^\infty\langle f|i(t)\rangle\times\exp[i(E_L+\epsilon_i)t/\hbar]\exp[-g(t)]dt\right|^2, \quad (2)$$

where E_L is the incident photon energy, E_S is the scattered photon energy, n is the solvent index of refraction, M is the transition length evaluated at the equilibrium geometry, P_i is the initial Boltzmann population of the ground-state energy level $|i\rangle$ which has energy ϵ_i, f is the final state for the resonance Raman process, and ϵ_f is the energy of the ground state energy level $|f\rangle$, and $\delta(E_L+\epsilon_i-E_S-\epsilon_f)$ is a delta function to add up cross sections with the same frequency. $|i(t)\rangle=e^{-iHt/\hbar}|i\rangle$ is $|i(t)\rangle$ propagated on the excited state surface for a time t. H is the excited state vibrational Hamiltonian. The $\exp[-g(t)]$ term in Eqs. (1) and (2) is a damping function. This is expected to be mostly direct photodissociation population decay with some solvent dephasing for *A*-band 1-bromo-2-iodoethane in cyclohexane. Addition over a ground state Boltzmann distribution of vibrational energy levels (298 K temperature distribution) was used to compute the absorption and resonance Raman cross sections. The number of initial vibrational energy levels included in the Boltzmann sum were up to $v=3$ for ν_{11}, $v=1$ for ν_9 and $v=0$ for ν_8, ν_7, ν_6, and ν_5.

The ground and excited state potential energy surfaces were approximated by harmonic oscillators displaced by Δ in dimensionless normal coordinates. We assumed the Condon approximation. The resonance Raman intensities of the first several overtones and combination bands are determined mostly by the slope of the excited state surface in the Franck–Condon region when no vibrational recurrences take place (as in a direct photodissociation). The featureless gas and solution phase *A*-band absorption spectra of 1-bromo-2-iodoethane suggests that the total electronic dephasing is mostly due to direct photodissociation prior to the first vibrational recurrence. The wave packet propagation was cut off after 40 fs so as to not to allow any significant recurrences of the wave packet to the Franck–Condon region. The $\langle f|i(t)\rangle$ overlaps decay and reach a negligible value after 30 fs for the resonance Raman peaks observed in our experimental spectra. Thus the cut-off at 40 fs just prevents the wavepacket to return to the Franck–Condon region and helps to better model a direct photodissociation reaction. The effects of solvent dephasing collisions on the absorption and resonance Raman cross sections were simulated by an exponential decay (the $\exp[-g(t)]$ term in Eqs. (1) and (2) was replaced by $\exp[-t\Gamma/\hbar]$). The bound harmonic oscillator model for the excited state used here only gives us a convenient way to simulate the region of the excited state that determines the resonance Raman intensities and absorption spectrum and does not imply the excited state is bound.

The potential parameters [in Eqs. (1) and (2)] are usually stated in terms of dimensionless normal coordinates. In order to easily visualize the short-time photodissociation dynamics in terms of bond length and bond angle changes, we converted the normal coordinate motions into internal coordinate motions. The center of the wave packet motion in terms of dimensionless normal coordinates at time t after excitation to the excited state (and undergoing separable harmonic dynamics) is given by

$$q_\alpha(t)=\Delta_\alpha(1-\cos\ \omega_\alpha t). \quad (3)$$

The time, t, is in units of fs, the vibrational frequency, ω_α, is in units of fs^{-1}, and we fix $q_\alpha=0$ for each mode α at the ground electronic state equilibrium geometry. At different times t the internal coordinate displacements are found from the dimensionless normal mode displacements $(q_\alpha(t))$,

$$s_i(t)=(h/2\pi c)^{1/2}\Sigma_\alpha A_{\alpha i}\varpi_\alpha^{-1/2}q_\alpha(t). \quad (4)$$

S_i are the displacements of the internal coordinates (bond stretches, bends, torsions, and wags as defined by Wilson, Decius, and Cross) from their ground electronic state equilibrium values. $A_{\alpha i}$ is the normal-mode coefficient $(\partial s_i/\partial Q_\alpha)$ with Q_α=the ordinary dimensioned normal coordinate. ϖ_α is the vibrational frequency in units of cm^{-1}. The normal coordinate analysis and vibrational assignments for 1-bromo-2-iodoethane have been recently reported[88] (see supplementary material[89]) and we made use of these results to compute the normal mode vectors of 1-bromo-2-iodoethane using a modified version of the Snyder and Schachtschneider FG program.[90] The Cartesian coordinates, complete force field, and normal-mode coefficients are available as supplementary material.[89]

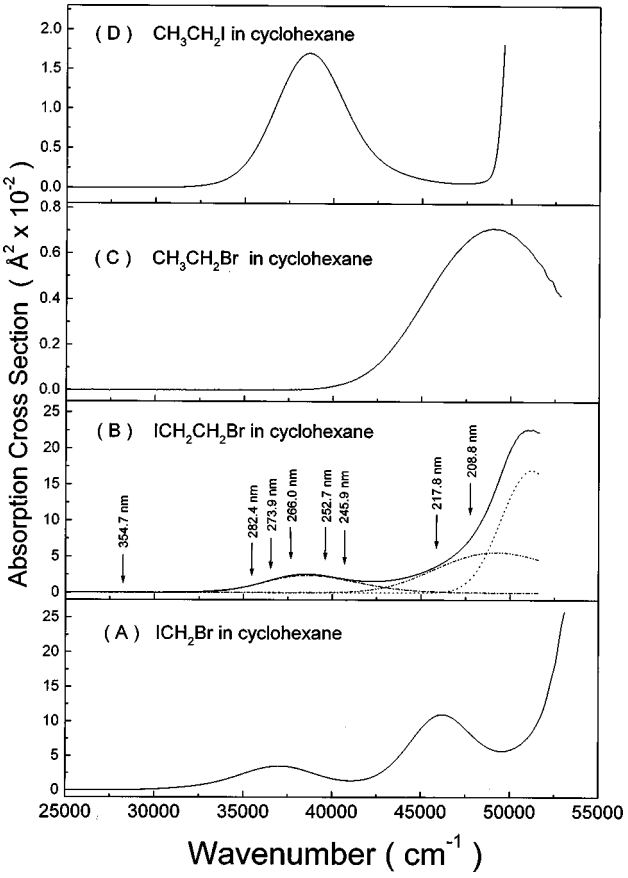

FIG. 1. Absorption spectra of bromoiodomethane (A), 1-bromo-2-iodoethane (B), bromoethane (C), and iodoethane (D) in cyclohexane solution. The excitation wavelengths (in nm) for the resonance Raman experiments are shown above the 1-bromo-2-iodoethane absorption spectrum.

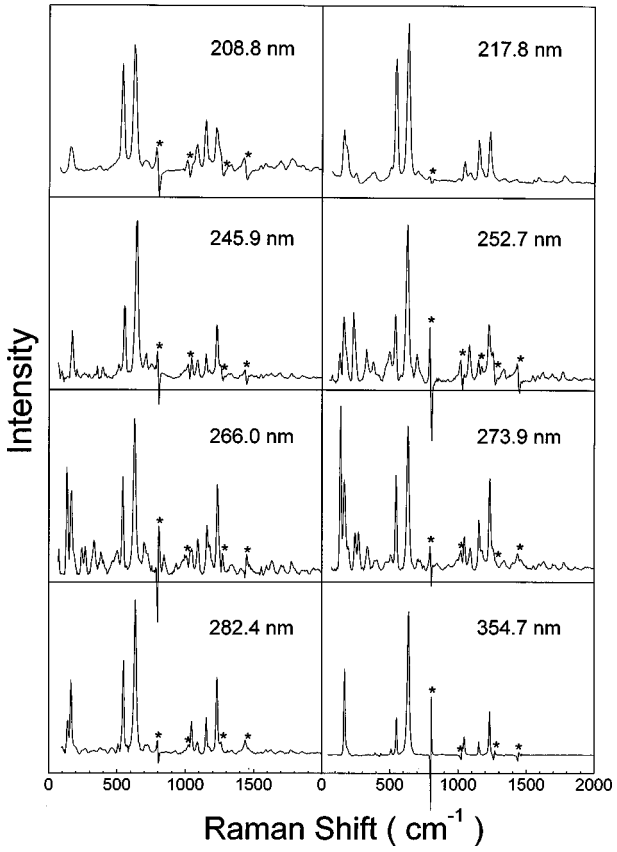

FIG. 2. Overview of the 1-bromo-2-iodoethane in cyclohexane solution resonance Raman spectra which have been intensity corrected and solvent subtracted. Asterisks (*) mark parts of the spectra where solvent artifacts are present and the pound sign (#) labels sections where a laser line or stray light artifact are present.

IV. RESULTS AND DISCUSSION

A. Absorption spectra

The absorption spectra of 1-bromo-2-iodoethane, bromoiodomethane, iodoethane, and bromoethane in cyclohexane solution are shown in Fig. 1. The *A*-band absorption of 1-bromo-2-iodoethane is associated with the C–I bond $n \rightarrow \sigma^*$ transitions similar to iodoethane and other iodoalkanes. However, the 1-bromo-2-iodoethane absorption band extinction coefficient maximum of 670 $cm^{-1}\,M^{-1}$ is substantially greater than the sum of the absorption coefficients of bromoethane (close to zero) and iodoethane (445 $cm^{-1}\,M^{-1}$) over the 280 nm to 240 nm region. This suggests that there is significant interaction of the C–I and C–Br chromophores in 1-bromo-2-iodoethane. The deconvolution of the *B*-band of 1-bromo-2-iodoethane shown in Fig. 1 displays contributions from two transitions that correlate well with the C–Br bond $n \rightarrow \sigma^*$ absorption spectrum found in bromoethane and the C–I Rydberg transitions around 200 nm in the iodoethane absorption spectrum.

B. Resonance Raman spectra

An overview of the resonance Raman spectra of 1-bromo-2-iodoethane in cyclohexane solution is displayed in Fig. 2. An expanded view of the 266.0 nm resonance Raman spectrum is shown in Fig. 3. The resonance Raman spectra of Figs. 2 and 3 have been intensity corrected and solvent subtracted. The *trans*-1-bromo-2-iodoethane resonance Raman bands have been tentatively assigned based on the nonresonant Raman and infrared spectra and vibrational assignments reported recently.[88] Table I lists the Raman shifts and intensities of the resonance Raman bands of 1-bromo-2-iodoethane for the *A*-band spectra shown in Fig. 3 for the region between 150 cm^{-1} and 2500 cm^{-1}. Most of the *A*-band resonance Raman peaks can be assigned to the fundamentals, overtones and/or combination bands of six Franck–Condon active vibrational modes of *trans*-1-bromo-2-iodoethane; ν_{11} (the nominal CCI bend), ν_9 (the nominal C–I stretch), ν_8 (the nominal C–Br stretch), ν_7 (the nominal C–C stretch), ν_6 (the nominal CH_2 wag with the iodine atom attached to the CH_2 group), and ν_5 (the nominal CH_2 wag with the bromine atom attached to the CH_2 group). The nominal C–I stretch overtone progression ($n\nu_9$) is the largest progression and forms significant combination bands with the other five Franck–Condon active modes.

The low frequency region of the resonance Raman spectra of 1-bromo-2-iodoethane displays some dependence on the excitation laser power (Raman bands labeled with an *A* in Fig. 3) and suggests the presence of a transient species formed during the laser pulse. Figure 4 shows a high and low power spectrum with a difference spectrum of the transient species. We did not observe any significant changes in the

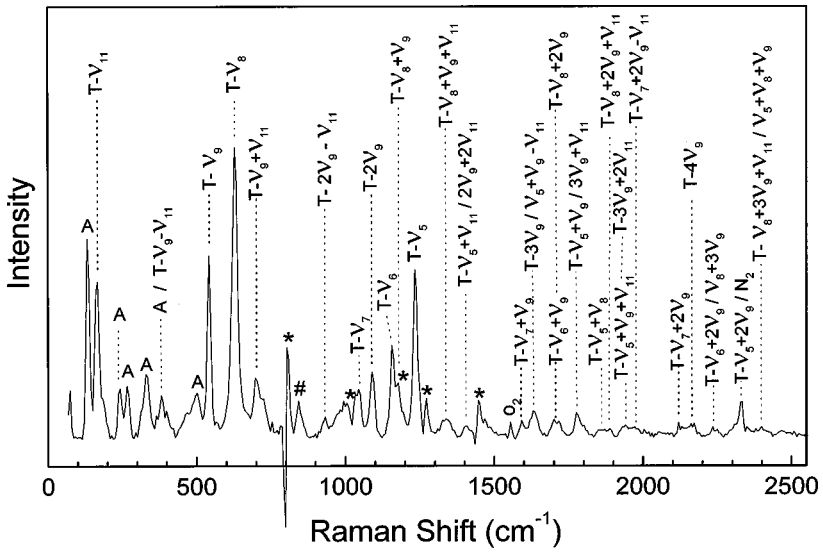

FIG. 3. Larger view of the 266.0 nm resonance Raman spectrum of 1-bromo-2-iodoethane in cyclohexane solution with tentative assignments of the more intense Raman bands labeled (T=*trans* conformer of 1-bromo-2-iodoethane) above the peaks in the spectrum. The resonance Raman spectrum has been intensity corrected and solvent subtracted. Regions of possible solvent subtraction artifacts are marked with asterisks (*) and the symbol A represents Raman bands due to an apparent transient species.

high and low power spectra above 800 cm^{-1}. The transient resonance Raman spectrum shown in Fig. 4 displays three Franck–Condon modes; a 144 cm^{-1} mode, a 174 cm^{-1} mode, and a 250 cm^{-1} mode. These three modes have noticeable intensity in their overtones and a few combination bands. The transient species could be a bromoethyl radical formed from the *A*-band photodissociation. The closely related CF_2CF_2Br radical[51] photodissociates at 248 nm and the

TABLE I. Experimental and calculated resonance Raman intensities for *trans*-1-bromo-2-iodoethane in cyclohexane solution.

		Intensities as absolute Raman cross sections ($\times 10^{-10}$ Å^2/molecule)									
		282.4 nm		273.9 nm		266.0 nm		252.7 nm		245.9 nm	
Raman bands	Raman shift[a] (cm^{-1})	Expt[b]	Calc[d]	Expt[b]	Calc[d]	Expt[b]	Calc[d]	Expt[b]	Calc[d]	Expt[b]	Calc[d]
ν_9	542	2.42	1.61	2.45	2.66	2.65	3.61	2.14	3.98	4.38	3.38
$2\nu_9$	1085	0.44	0.69	0.88	1.17	1.29	1.59	2.10	1.73	1.76	1.45
$3\nu_9$ / $\nu_5+\nu_9-\nu_{11}$	1630	0.28	0.35	0.57	0.59	0.98	0.80	0.64	0.87	0.82	0.73
$4\nu_9$ / $\nu_7+2\nu_9$	2171	0.26	0.27	0.51	0.49	0.65	0.56	0.88	0.72	0.46	0.58
ν_5	1233	2.03[c]	0.26	1.97[c]	0.46	2.84[c]	0.66	1.99[c]	0.80	4.08[c]	0.71
$\nu_5+\nu_9$ / $\nu_{11}+3\nu_9$	1775	0.30	0.25	0.41	0.42	0.64	0.61	0.58	0.73	0.61	0.65
$\nu_5+2\nu_9$	2332	0.19	0.15	0.26	0.29	0.39	0.37	0.88	0.48	0.54	0.40
$\nu_5+\nu_{11}$ /$2\nu_9+2\nu_{11}$	1409	0.15	0.08	0.20	0.14	0.20	0.18	0.18	0.19	0.14	0.16
ν_6	1155	0.85	0.10	0.94	0.16	3.35	0.23	1.24	0.27	1.55	0.24
$\nu_6+\nu_9$	1697	0.14	0.08	0.17	0.13	0.24	0.19	0.35	0.23	0.79	0.20
$\nu_6+2\nu_9$ / $\nu_8+3\nu_9$	2254	0.10	0.08	0.17	0.10	0.23	0.21	0.34	0.44	0.21	0.20
ν_8	630	5.43	0.17	4.81	0.29	5.51	0.39	7.65	0.44	14.7	0.37
$\nu_8+\nu_9$	1176	0.23[c]	0.15	0.65[c]	0.25	0.96[c]	0.35	0.88[c]	0.38	0.29[c]	0.32
$\nu_8+\nu_9+\nu_{11}$	1330	0.10	0.04	0.20	0.07	0.22	0.09	0.28	0.10	0.19	0.08
$\nu_5+\nu_8$	1863	0.10	0.09	0.15	0.15	0.25	0.21	0.23	0.23	0.45	0.19
$\nu_5+\nu_8+\nu_9$	2411	0.05	0.07	0.07	0.09	0.10	0.13	0.20	0.16	0.14	0.14
$\nu_8+2\nu_9$	1716	0.14	0.10	0.20	0.17	0.30	0.23	0.25	0.26	0.20	0.21
ν_7	1044	0.76[c]	0.15	0.76[c]	0.26	0.95[c]	0.37	...[c]	0.44	0.96[c]	0.38
$\nu_7+\nu_9$	1592	0.19	0.12	0.14	0.21	0.37	0.30	0.41	0.35	0.38	0.31
ν_{11}	160	1.77	0.32	2.77	0.52	2.25	0.68	2.20	0.70	2.92	0.58
$2\nu_{11}$	315	0.05	0.02	0.15	0.03	0.20	0.04	0.15	0.04	0.15	0.03
$\nu_{11}+\nu_9$	708	0.20	0.28	0.35	0.46	0.68	0.60	1.09	0.61	1.08	0.49
$\nu_9-\nu_{11}$	388	0.20[c]	0.13	0.23[c]	0.20	0.28[c]	0.26	0.31[c]	0.25	0.25[c]	0.20
$\nu_5+\nu_9+\nu_{11}$ /$2\nu_{11}+3\nu_9$	1941	0.07	0.11	0.24	0.20	0.22	0.23	0.32	0.28	0.23	0.19

[a]Estimated uncertainties are about ± 4 cm^{-1} for the Raman shifts.

[b]Intensities are based on integrated areas of peaks and absolute Raman cross section measurements (the listed values are in units of 10^{-10} Å^2/molecule). Estimated uncertainties are about 10% for intensities for 1.0 or higher, 15% for intensities 0.3 to 1.0, and 25% for intensities lower than 0.3.

[c]These peaks are obscured by solvent subtraction artifacts and/or apparent transient Raman peaks and therefore these bands higher uncertainties for their integrated areas.

[d]The parameters of Table II and the model described in Sec. III are used to calculate the *A*-band Raman intensities.

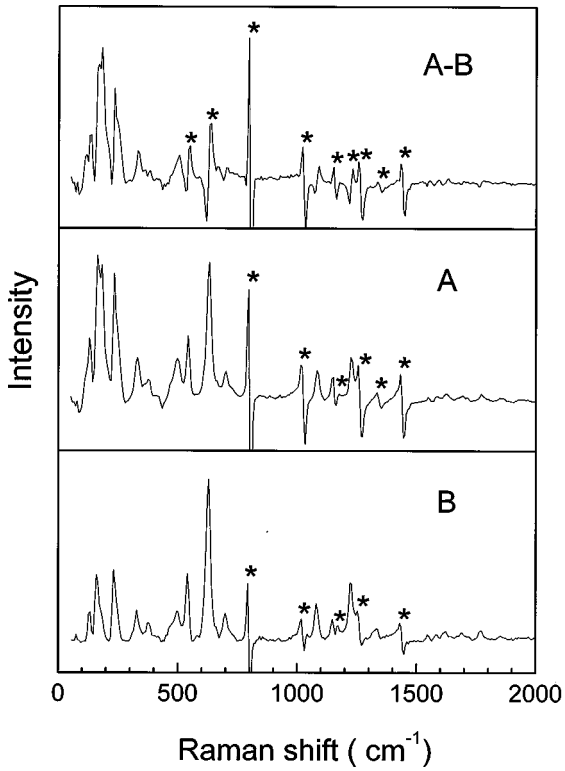

FIG. 4. High power 252.7 nm resonance Raman spectrum (A) and low power 252.7 nm resonance Raman spectrum (B) of 1-bromo-2-iodoethane in cyclohexane solution. The difference spectrum of A–B shows some features that may be due to a resonance Raman spectrum of a transient species.

CF_2BrCH_2 radical[91] photodissociates at 248 nm and 266 nm and this suggests that the bromoethyl radical would also have an absorption band in this region. The strength of the bromoethyl radical absorption band would also be expected to be substantially larger than the parent 1-bromo-2-iodoethane molecule (670 $M^{-1}\,cm^{-1}$ or 2.56×10^{-18} cm^2/molecule) since other related haloalkyl radicals[92,93] such as chloromethylene and bromomethylene have large *A*-band absorptions (14.5×10^{-18} cm^2/molecule for the CH_2Cl radical and 8.8×10^{-18} cm^2/molecule for the CH_2Br radical).[92,93] If the bromoethyl radical has a similar absorption cross section then its Raman cross section could be 12 to 32 times larger than that for the parent 1-bromo-2-iodoethane. In addition, the Raman cross section for the transient compound appears distributed over fewer bands compared to the 1-bromo-2-iodoethane resonance Raman spectra which could cause the Raman cross section per Raman band to appear relatively larger and increase our sensitivity to the bromoethyl photoproduct. Thus, a few percent of bromoethyl radicals being formed in the experiment could give rise to the transient bands in the 252.7 nm, 266.0, 273.9 nm resonance Raman spectra. We have estimated an upper limit for the fraction of sample photoconverted to be about 4.7% for 266 nm under the conditions used for collecting the resonance Raman spectra shown in Figs. 2 and 3. This estimate was determined using the following equation from Ref. 87:

$$F_{\text{pulse}}=(2303E\epsilon\phi)/(\pi r^2 N_A) \tag{5}$$

TABLE II. Parameters for the calculation of resonance Raman intensities and absorption spectrum of *trans*-1-bromo-2-iodoethane in cyclohexane solution.[a]

Vibrational mode	Ground state frequency (cm^{-1})	Excited state frequency (cm^{-1})	$\lvert\Delta\rvert$
ν_{11} (CCI bend)	160	160	5.6
ν_9 (C–I stretch)	548	548	4.85
ν_8 (C–Br stretch)	630	630	1.4
ν_7 (C–C stretch)	1044	1044	0.85
ν_6 (CH_2^* wag)[b]	1155	1155	0.61
ν_5 (CH_2 wag)	1233	1233	0.98

[a]Transition length, $M=0.245$ Å; $E_0=27\,930\ cm^{-1}$; $\Gamma=50\ cm^{-1}$.
[b]* represents the CH_2 group that has the iodine atom attached to it. The other CH_2 group has the Br atom attached to it.

and these conditions for 266 nm excitation; 1.0 mW at 10 Hz$=1\times10^{-4}$ J$=1.34\times10^{14}$ photons for 266 nm light so $E=1.34\times10^{14}$ photons, $r=0.05$ cm, $\epsilon=720$ $M^{-1}\,cm^{-1}$, $\phi=1.0$, and $N_A=6.02\times10^{23}$. The less than 5% photoconversion upper limit is consistent with the absolute resonance Raman cross section experimental measurements that showed no significant ground state depletion (e.g., changes of less than 5% for powers between 0.2 mW to 1.50 mW). We note that molecular beam studies of the *A*-band photodissociation of CF_2BrCF_2I showed that stable CF_2CF_2Br radicals could be formed, but there were no stable CH_2CH_2Br products observed from the CH_2BrCH_2I photodissociation.[94] However, Br atom products were observed from the CH_2BrCH_2I photodissociation and it was suggested that they come from secondary dissociation of the bromoethyl radical.[94] The CH_2CH_2Br radical could be stabilized in a solution environment which could allow it to absorb a second photon and account for the transient we observe in our high power spectrum. Further experimental and theoretical work needs to be done to unambiguously identify the apparent transient resonance Raman spectrum we observe at higher excitation laser powers. Apart from the several transient resonance Raman bands, the resonance Raman intensities and absolute cross section measurements given in Table I should be indicative of the parent 1-bromo-2-iodoethane molecule. In order to learn more quantitative information on the short-time dynamics of 1-bromo-2-iodoethane, we have carried out a resonance Raman intensity analysis which is detailed in the following sections.

C. Modeling of the absorption and resonance Raman spectra

The parameters shown in Table II were used in Eqs. (1) and (2) of Sec. III to model the absorption spectrum and resonance Raman intensities of *trans*-1-bromo-2-iodoethane. We fit the intensities of the overtones and combination bands but did not try to fit the fundamental intensities because fundamental bands in many *A*-band resonance Raman spectra of iodoalkanes are prone to preresonant-resonant interference effects from higher energy excited electronic states.[29,33,67,73,77] In addition, we also put more emphasis on fitting intensities of the resonance Raman spectra with excitation wavelengths near the peak of the absorption band

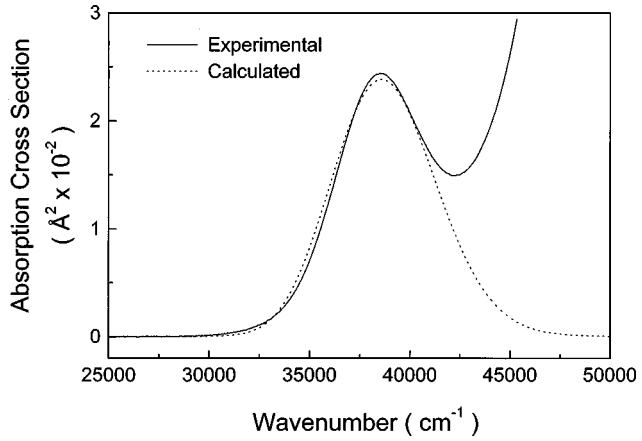

FIG. 5. Comparison of the calculated (dashed line) and the experimental absorption (solid line) of 1-bromo-2-iodoethane in cyclohexane solution in the A-band region. The parameters of Table II were used in Eq. (1) and the model described in Sec. III to compute the calculated absorption spectrum.

since these resonance Raman spectra are less likely to have any significant contributions to their intensities from the usually weak $^1Q_1$ and $^3Q_1$ transitions near the blue and red edges of the absorption spectra of iodoalkanes.

Figure 5 displays a comparison of the calculated and experimental absorption spectra. The calculated spectrum shows fairly good agreement with the experimental spectrum considering that the *trans* conformer accounts for about 70% of the 1-bromo-2-iodoethane in cyclohexane solution at room temperature and the probable presence of small $^1Q_1$ and $^3Q_1$ transitions at the red and blue edges of the absorption spectrum. We found the intensity of the C–I stretch mode for the *gauche* conformer (G-ν_9, ~504 cm^{-1}) to be much smaller than expected compared to the corresponding mode of the *trans* conformer (T-ν_9, ~542 cm^{-1}) in the 282.4 nm resonance Raman spectrum (resonant with the *A*-band and little affected by the transient bromoethyl bands) and the preresonant 354.7 nm Raman spectrum. The C–I stretch mode for the gauche conformer had about 7%–8% of the C–I stretch resonance Raman intensity at 282.4 nm and about 13% at 354.7 nm compared to the expected 30% observed in the nonresonant FT-Raman spectrum with 1064 nm. This suggests that the *A*-band absorption coefficient and resonance Raman enhancement are very different for the *trans* and *gauche* conformers of 1-bromo-2-iodoethane. The *trans* conformer has the C–I and C–Br chromophores in the same plane and parallel to one another which is favorable to significant interaction between them. However, the C–I and C–Br chromophores are not in the same plane and are not parallel in the *gauche* conformer and this likely leads to negligible interaction between the chromophores. The *gauche* conformer of 1-bromo-2-iodoethane probably has an *A*-band absorption coefficient very similar to that for iodoethane (445 M^{-1} cm^{-1}). If we assume that the 1-bromo-2-iodoethane gauche conformer has an absorption coefficient like iodoethane, we can estimate the *trans* conformer *A*-band absorption coefficient to be about 766 M^{-1} cm^{-1} [1-bromo-2-iodoethane total absorption=670 M^{-1} cm^{-1}=0.7 (*trans* absorption coefficient +0.3 (445 M^{-1} cm^{-1})]. The resonance Raman cross sections for the two conformers will scale approximately by the square of the absorption coefficients to give a factor of ~3 times more enhancement for the *trans* conformer relative to the *gauche* conformer. This would lead to about 10% of the resonance Raman intensity going into the *gauche* conformer bands which is similar to the 7%–8% we observe for the C–I stretch mode for the *gauche* conformer (G-ν_9, 504 cm^{-1}) in the 282.4 nm resonance Raman spectrum. Other *gauche* Raman bands are difficult to unambiguously discern in the resonance Raman spectra since they are very small and nearly coincident with many of the *trans* Raman bands. The small amount of apparent resonance Raman intensity (~8%) and absorption intensity (~18%) of the *gauche* conformer will lead us to slightly underestimate the actual *trans*-1-bromo-2-iodoethane absolute Raman cross sections by ~10% to give a bit more uncertainty to these measurements.

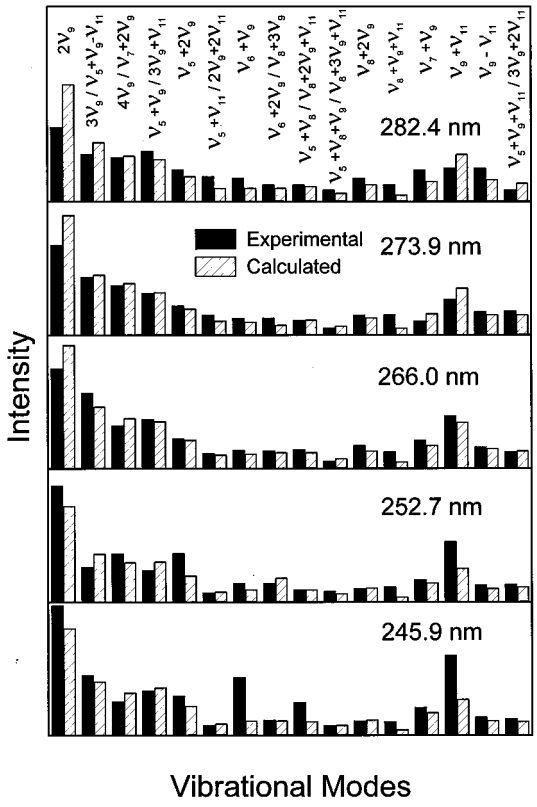

FIG. 6. Comparison of experimental (solid bars) and calculated (open bars) resonance Raman cross sections for the 282.4 nm, 273.9 nm, 266.0 nm, 252.7 nm, and 245.9 nm *A*-band resonance Raman spectra of 1-bromo-2-iodoethane in cyclohexane solution. The parameters given in Table II and the model described in Sec. III were used in conjunction with Eq. (2) to calculate the resonance Raman cross sections.

A comparison of the calculated and experimental resonance Raman cross sections of *trans*-1-bromo-2-iodoethane is given in Fig. 6 and Table I. There is reasonable agreement between most of the Raman intensities for the combination bands and overtones (see Fig. 6 and Table I). However, there were large disagreements for several of the fundamental intensities such as ν_5, ν_6, ν_7, ν_8, and ν_{11} and this is probably due to these fundamental peaks having significant preresonant enhancement from higher energy excited states. This view is also supported by the higher energy resonance Raman spectra (see the 217.8 nm and 208.8 nm spectra in Fig.

2) which have strong intensity in these fundamentals. This is not too surprising since the fundamentals of *A*-band resonance Raman spectra of other iodoalkanes have also displayed significant preresonant contributions from higher energy excited states while the intensities of the combination bands and overtones are relatively unaffected.[29,33,67,73,76] As one tunes off resonance with the higher energy excited states, the overtone and combination band intensities decrease very rapidly compared to the fundamental intensities. The *A*-band absorption is relatively far away from the other higher energy excited states ($>10\,000$ cm^{-1}) and therefore only the preresonant fundamental intensities are strong enough to be noticed in the *A*-band resonance Raman spectra.

Taking into account the simple model and approximations used in our simulations, the overall agreement between the calculated and experimental resonance Raman cross sections (for the overtones and combination bands) and absorption spectra is fairly good. Table II lists the best fit normal mode displacement parameters (Δ) for the simulations and these parameters are given in terms of dimensionless normal coordinates. The dimensionless normal coordinate displacements (Δ) can be converted into internal coordinate changes as a function of time so as to examine the *A*-band short-time photodissociation dynamics of *trans*-1-bromo-2-iodoethane.

D. Short-time photodissociation dynamics of *trans*-1-bromo-2-iodoethane and comparison to other dihaloalkanes

The normal mode descriptions of the *trans*-1-bromo-2-iodoethane Franck–Condon active modes were used in Eqs. (3) and (4) to determine the short-time photodissociation dynamics in terms of internal coordinate motions. We have picked 10 fs as the time to examine the short-time photodissociation dynamics because the $\langle f|0(t)\rangle$ overlaps which determine the resonance Raman cross sections usually reach their maxima about 5–10 fs after photoexcitation and the 10 fs time allows convenient comparison to previous work on related dihaloalkanes. Since the resonance Raman intensity analysis only provides the magnitude but not the sign of the Franck–Condon active normal mode displacement, there are 2^n possible sign combinations that will be equally consistent with the results of the resonance Raman intensity analysis. For more information on the difficulty of picking the signs of the normal mode displacements, the reader is referred to a couple of recent review articles.[86,87]

Because we know that *A*-band photoexcitation leads to direct C–I bond cleavage, we shall assume that the C–I bond becomes lengthened upon photoexcitation. This reduces the number of possible sign combinations of the normal mode displacements by one-half. Since the CCI angle almost always becomes smaller for the *A*-band short-time photodissociation dynamics of iodoalkanes[67,76,78] and most dihaloethanes[77,79] investigated so far, we shall also assume that the CCI angle becomes smaller for the *A*-band short-time photodissociation dynamics of *trans*-1-bromo-2-iodoethane. Using the two preceding assumptions about the C–I bond and CCI angle, we are left with $2^4=16$ possible sign combinations and their associated geometry changes. We divide these 16 possible sign combinations into two sets of ranges of geometry changes; the first set of geometry changes have the C–Br bond becoming longer and the second set of geometry changes have the C–Br bond becoming smaller. Table III lists the two sets of internal coordinate displacements at 10 fs after photoexcitation for *trans*-1-bromo-2-iodoethane. Table III also compares the short-time photodissociation dynamics for *trans*-1-bromo-2-iodoethane with iodoethane, *trans*-1-chloro-2-iodoethane and *trans*-1,2-diiodoethane. Figure 7 presents simplified geometries for *trans*-1-bromo-2-iodoethane, iodoethane, *trans*-1-chloro-2-iodoethane, and *trans*-1,2-diiodoethane which can be used to aid in visualizing the internal coordinate changes given in Table III. In Fig. 7 and Table III, C represents the α-carbon atom to which the iodine atom is attached and B represents the β-carbon atom attached to the α-carbon atom.

The results of Table III show that 1-bromo-2-iodoethane has significant bond length changes in both the C–I and C–Br bonds in the Franck–Condon region of the photodissociation reaction. The C–C bond also has a broad range of most probable displacements at 10 fs and the CCBr angle becomes smaller. The HCB, ICH, CBH, and HBBr angles have a broad range of most probable displacements at 10 fs while the C–H bond and the HCH and HBH angles do not change very much in comparison to the changes found for other bond lengths and bond angles. These dynamics suggests that the hydrogen atoms and C–H bonds are relatively rigid during the Franck–Condon region dynamics while the carbon and halogen atoms attached to the C–C, C–I, and C–Br bonds experience most of the dynamical changes associated with the initial stages of the photodissociation. If the C–Br bond becomes longer (set A range of displacements at 10 fs in Table III) then the C–B bond length, BCI angle, CBBr angle shift to noticeably more negative values than in the case for the C–Br bond becoming smaller (set B range of displacements at 10 fs in Table III). The short-time photodissociation dynamics for 1-bromo-2-iodoethane shown in Table III suggest that the photodissociation reaction has a significant multidimensional character with the C–I bond breaking occurring on a time scale similar to the vibrational motions of the rest of the molecule. The Table III dynamics for 1-bromo-2-iodoethane also suggest that significant internal excitation of the bromoethyl photofragment occurs in the lower frequency vibrational modes associated with the C–C and C–Br bonds and the HCB, CBH, and HBBr angles in so far as the initial photodissociation dynamics determines the internal excitation of the photofragments.

It is interesting to compare our short-time photodissociation dynamics for 1-bromo-2-iodoethane with those found for iodoethane, 1-chloro-2-iodoethane, and 1,2-diiodoethane (see Table III). Inspection of Table III shows some trends in the Franck–Condon region photodissociation dynamics as a β-hydrogen atom on iodoethane is replaced by more massive halogen atoms (Cl and I). As the molecule is changed from iodoethane to 1-chloro-2-iodoethane and finally to 1,2-diiodoethane, the C–I bond length changes generally proceed from a fairly long and narrow range of $+0.13$ to $+0.15$ Å at 10 fs for iodoethane to broader ranges and shorter bond length changes for 1,2-diiodoethane ($+0.068$ to $+0.116$ Å and $+0.033$ to $+0.068$ Å for the two C–I bonds). There is

TABLE III. Most probable *A*-band internal coordinate displacements of *trans*-1-bromo-2-iodoethane at $t = 10$ fs assuming the C–I bond becomes longer and the CCI angle becomes smaller. Comparison to previous results for iodoethane, *trans*-1-chloroethane and *trans*-1,2-diiodoethane.

Trans-1-bromo-2-iodoethane (this work)			
Set A (the C–Br bond becomes longer)		Set B (the C–Br becomes shorter)	
Coordinate	Range of displacements at $t = 10$ fs	Coordinate	Range of displacements at $t = 10$ fs
r_{CI}	+0.115 to +0.196 Å	r_{CI}	+0.115 to +0.196 Å
r_{CBr}	+0.013 to +0.094 Å	r_{CBr}	−0.102 to −0.021 Å
r_{BC}	−0.145 to +0.047 Å	r_{BC}	−0.115 to +0.077 Å
r_{CH}	$<\pm$0.006 Å	r_{CH}	$<\pm$0.006 Å
∠BCI	−11.3° to −3.3°	∠BCI	−7.6° to +0.5°
∠HCB	−10° to +11.6°	∠HCB	−11° to +10.6°
∠ICH	−8.1° to +13.6°	∠ICH	−8.8° to +12.9°
∠CBBr	−11.9° to −3.4°	∠CBBr	−8.2° to +0.2°
$\angle CBH_{7\text{ or }8}$	−11.2° to +16°	$\angle CBH_{7\text{ or }8}$	−11.3° to +14.8°
∠HCH	−1.2° to +1.9°	∠HCH	−1.6° to +1.9°
∠HBH	−1.9° to +2.5°	∠HBH	−1.8° to +2.6°
∠HBBr	−13.2° to +14.2°	∠HBBr	−13.8° to +13.6°
1-Chloro-2-Iodoethane (from Ref. 77)		Iodoethane (from Ref. 67)	
r_{CI}	+0.09 to +0.18 Å	r_{CI}	+0.13 to +0.15 Å
r_{CCI}	−0.01 to −0.18 Å		
r_{BC}	−0.024 to +0.012 Å	r_{BC}	−0.06 to −0.05 Å
r_{CH}	$<\pm$0.004 Å	r_{CH}	$<\pm$0.004 Å
∠BCI	−7.8° to +2.5°	∠BCI	−6° to −3°
∠HCB	−0.8° to +0.8°	∠HCB	+6° to +9°
∠ICH	−0.4° to +2.5°	∠ICH	−7° to −3°
∠CBCl	−8.8° to +3.2°	$\angle CBH_8$	−1° to +5°
$\angle CBH_{7\text{ or }8}$	−0.7° to +2°	$\angle CBH_{7\text{ or }6}$	−3° to −1°
∠HCH	−0.6° to +1°	∠HCH	−6° to +5°
∠HBH	−0.2° to +1.1°	$\angle H_7BH_6$	−8° to +8°
∠HBCl	−0.8° to +1.4°	$\angle H_8BH_{7\text{ or }6}$	−4° to +5°
1,2-Diiodoethane (from Ref. 79)			
first r_{CI}	+0.068 to +0.116 Å		
second r_{CI}	+0.033 to +0.068 Å		
r_{CC}	−0.138 to +0.071 Å		
r_{CH}	$<\pm$0.005 Å		
∠CCI	−8.7° to −1.8°		
∠HCC	−6.8° to +7.6°		
∠ICH	−4.6° to +7.8°		
∠HCH	0.0° to +2.5°		

also a similar trend in the C–C bond length changes from a narrower to a broader range of displacements in going from iodoethane (−0.05 to −0.06 Å) to 1,2-diiodoethane (−0.138 to +0.071 Å). These trends in the C–I and C–C bond length changes in the *A*-band short-time photodissociation dynamics for the dihaloethanes suggest that as the haloethyl group becomes more massive there is more internal excitation of the haloethyl radical in so far as the initial photodissociation dynamics determines the energy partitioning. This is similar to trends found for the C–I bond length short-time dynamics of iodoalkanes as the alkyl group becomes more massive and/or branched.[67,75,76] The trends in the C–I and C–C bond lengths for iodoethane, 1-chloro-2-iodoethane, and 1,2-diiodoethane also correlate well with the results of time-of-flight translational spectroscopy experiments which show that for iodoethane approximately 32%–39% of the available energy goes into internal excitation of the ethyl radical photoproduct,[12,16] for 1-chloro-2-iodoethane about 42%–54% of the available energy goes into internal excitation of the chloroethyl radical,[50] and for 1-bromo-2-iodoethane about 53%–58% of the available energy goes into internal excitation of the bromoethyl radical.[94] However, the short-time dynamics for 1-bromo-2-iodoethane in Table III show the C–I bond lengths do not change very much in going from 1-chloro-2-iodoethane (+0.09 to +0.18 Å at 10 fs) to 1-bromo-2-iodoethane (+0.115 to +0.196 Å at 10 fs) but the C–C bond length changes are substantially greater for 1-bromo-2-iodoethane (−0.145 to +0.077 Å at 10 fs) than for 1-chloro-2-iodoethane (−0.024 to +0.012 Å at 10 fs), and very similar to those found for 1,2-diiodoethane (−0.138 to +0.071 Å at 10 fs). Why are the C–C bond length changes for the short-time photodissociation dynamics for 1-bromo-2-iodoethane and 1,2-diiodoethane very similar to one another and very different from those found previously for iodoethane and 1-chloro-2-iodoethane?

In order to help elucidate the trends observed for the 1,2-dihaloethane short-time dynamics shown in Table III, it is useful to also examine the corresponding trends in the *A*-band absorption spectra. The *A*-band maximum absorption coefficients in cyclohexane solution are 445 $cm^{-1}\,M^{-1}$ for iodoethane, 490 $cm^{-1}\,M^{-1}$ for 1-chloro-2-iodoethane, 670 $cm^{-1}\,M^{-1}$ for 1-bromo-2-iodoethane and 1930 $cm^{-1}\,M^{-1}$

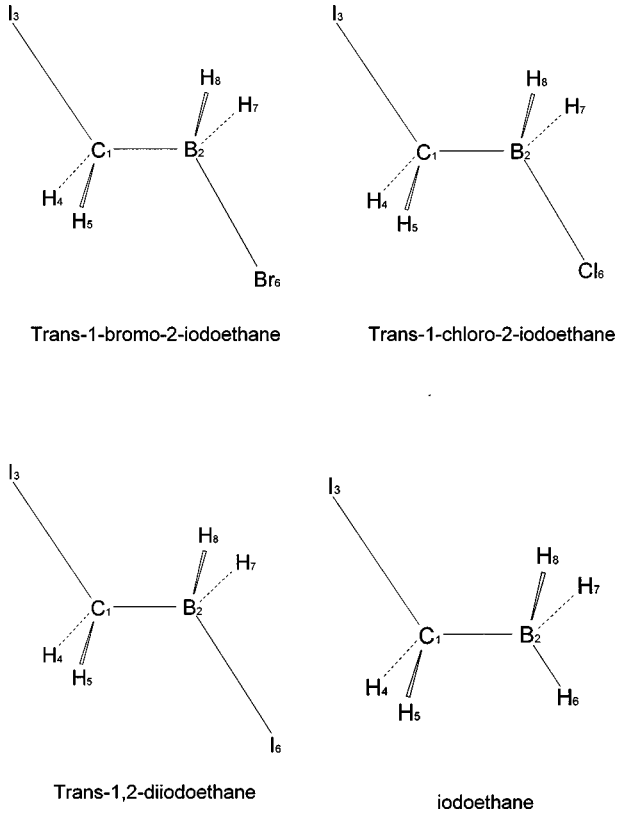

FIG. 7. Simplified geometries of the ground electronic state *trans*-1-bromo-2-iodoethane, *trans*-1-chloro-2-iodoethane, *trans*-1,2-diiodoethane, and iodoethane. These can be used in conjunction with Table III to help visualize the short-time photodissociation dynamics.

for 1,2-diiodoethane. The *A*-band absorptions for iodoethane and 1-chloro-2-iodoethane have very similar absorption coefficients and appear to be predominantly due to the C–I bond alone. However, there is a substantial increase in the absorption coefficients for 1-bromo-2-iodoethane and 1,2-diiodoethane that cannot be accounted for by simple addition of the iodoethane absorption plus bromoethane absorption for 1-bromo-2-iodoethane or the addition of two iodoethane chromophores for 1,2-diiodoethane. This additional increase in the absorption coefficients above the nominal simple addition of single chromophores is presumably due to significant interaction between the two carbon–halogen chromophores in 1-bromo-2-iodoethane and 1,2-diiodoethane. Excitation within the *A*-band absorption for 1-bromo-2-iodoethane and 1,2-diiodoethane would likely excite both carbon halogen chromophores to some extent. The two carbon atoms of the 1,2-dihaloethane molecule would then experience noticeable forces from the halogen atoms. Whether these forces are opposing or not opposing each other, they will strain the carbon–carbon bond and probably give rise to larger and broader range of displacements for the C–C bond in the haloethyl radical photofragment. This is consistent with the short-time photodissociation we observe for 1-bromo-2-iodoethane and 1,2-diiodoethane in Table III. The substantially larger C–C displacements observed for the short-time photodissociation dynamics of 1-bromo-2-iodoethane and 1,2-diiodoethane is probably due to simultaneous excitation of the two carbon halogen bonds to some degree.

The *A*-band short-time photodissociation dynamics for iodoethane[67] show that the structure of the ethyl group changes closer to a planar structure about the α-carbon atom similar to the structure of the ethyl radical and this suggests there is little internal excitation of the ethyl radical photoproduct in so far as the initial dynamics determine the internal excitation of the ethyl radical. *Ab initio* work[95,96] has shown the ethyl radical C–C bond length is about 1.49 Å and the iodoethane C–C bond length is 1.54 Å for their ground electronic states. Thus, the short-time dynamics for iodoethane *A*-band photodissociation brings the C–C bond length toward the ethyl radical structure and this suggests there is not much excitation of the C–C bond in the ethyl photofragment. The 1-chloro-2-iodoethane *A*-band short-time dynamics do not change towards a more planar structure about the α-carbon as much as the iodoethane and this may result in more internal excitation of the chloroethyl radical in so far as the initial photodissociation dynamics determines the internal excitation of the photofragments.[77] The 1-chloro-2-iodoethane *A*-band short-time dynamics in Table III show that the C–C bond length does not change much but the C–Cl bond length becomes significantly shorter. This could be mostly due to the C–I bond breaking pushing the C–C group toward the massive chlorine atom and not due to significant photoexcitation of the C–Cl chromophore. Since the 1-chloro-2-iodoethane *A*-band absorption coefficient is very similar to that of iodoethane there is most likely not much interaction of the C–I and C–Cl chromophores and one would not expect much direct excitation of the C–Cl bond when the *A*-band associated with the C–I bond is excited.

It is interesting to note that the *A*-band short-time photodissociation results for 1-chloro-2-iodoethane and 1-bromo-2-iodoethane show some correlation with the ability to observe stable haloethyl radicals in molecular beam experiments produced from *A*-band photoexcitation reactions. Our results for 1-chloro-2-iodoethane indicate that there is probably little direct photoexcitation of the C–Cl bond and that it likely receives some displacement from the kinematics of the C–I bond cleavage and the chloroethyl radical fragment is readily observed in molecular beam experiments.[91] However, our results suggest that the both the C–I and C–Br bonds receive some direct photoexcitation due to some interaction of the C–I and C–Br chromophores in 1-bromo-2-iodoethane and the bromoethyl radical is not directly observed in molecular beam experiments done with *A*-band photoexcitation.[92] Addition of fluorine atoms to stabilize the radical enables the molecular beam experiments to directly observe CF_2CF_2Br and CF_2CF_2I radicals from the *A*-band photodissociation reactions of ICF_2CF_2Br and ICF_2CF_2I, respectively.[94]

Our studies of the dihaloethanes (1-chloro-2-iodoethane, 1-bromo-2-iodoethane, and 1,2-diiodoethane) indicate that substitution of a hydrogen atom attached to the β-carbon of iodoethane by a more massive halogen atom results in significant substituent effects on the *A*-band short-time photodissociation dynamics. The 1,2-dihaloethane examined so far exhibit multidimensional dynamics with the C–I bond break-

ing occurring on a similar time scale as vibrational motion in the rest of the molecule. The short-time dynamics of the dihaloethanes appear to be somewhere in-between the simple ''rigid radical'' and ''soft radical'' descriptions of the photodissociation dynamics. The dihaloethanes (1-chloro-2-iodoethane, 1-bromo-2-iodoethane, and 1,2-diiodoethane) investigated showed noticeable bond length changes in the secondary carbon–halogen bond during the *A*-band short-time photodissociation dynamics due to kinematics and/or simultaneous excitation of both C–X chromophores. The degree of changes in the C–C bond length during the *A*-band short-time photodissociation dynamics for the 1,2-dihaloethanes shows a good correlation with the amount of enhancement of the *A*-band absorption extinction coefficients due to interaction of the C–X chromophores.

Our present resonance Raman intensity analysis study of 1-bromo-2-iodoethane is intended to provide a modest beginning to elucidate the bond breaking dynamics. The short-time dynamics that we derive from the resonance Raman intensity analysis depend on the ground state normal description and several other factors that are either ambiguous or not completely certain. The normal mode description currently used for 1-bromo-2-iodoethane is based on one isotopic derivative and a force field similar to those used in other dihaloethanes. The lower frequency modes associated with the halogen and carbon atoms (ν_{11}, ν_9, ν_8, and ν_7) determine most of the associated short-time photodissociation presented here for 1-bromo-2-iodoethane. As the normal mode descriptions are changed moderately for these low frequency vibrations, the main features of the short-time dynamics associated with the Br, I, and carbon atoms do not change very much. As long as the normal mode descriptions for the Franck–Condon active modes are not greatly inaccurate, the basic features of the short-time dynamics for 1-bromo-2-iodoethane should be reasonably semiquantitative. The accuracy of the normal mode descriptions can be improved using vibrational data from several isotopic derivatives to better refine the force field. We have assumed that the relative contributions of the $^3Q_0$, $^1Q_1$, and $^3Q_1$ states are similar to those previously found for other iodoalkanes in their *A*-band absorption spectra (e.g., the $^3Q_0$ contributes 70%–80% of the oscillator strength and accounts for most of the *A*-band resonance Raman intensity). A magnetic circular dichroism (MCD) experiment or another appropriate experiment is needed to ascertain the actual relative contribution of these three transitions in the 1-bromo-2-iodoethane *A*-band absorption and how this may be influenced by the C–Br chromophore. Solvation effects have generally been found to be relatively small for the *A*-band resonance Raman spectra and associated short-time photodissociation dynamics of most iodoalkanes and dihaloalkanes studied in both gas and solution phases (iodomethane,[27–33] iodoethane, 2-iodopropane, and 2-methyl-2-iodopropane,[65–68] and chloroiodomethane[97]). We expect that solvation effects are also fairly small for 1-bromo-2-iodoethane *A*-band resonance Raman spectra and short-time photodissociation dynamics although a comparison to a gas phase study is needed to verify this. Substantial solvation effects on the *A*-band resonance Raman spectra for room temperature liquid phase iodoalkanes has so far only been observed (to our knowledge) for diiodomethane where solvent induced symmetry breaking occurs along the ICI reaction coordinate.[72] The preceding uncertainties in the exact nature of the ground state normal mode descriptions, the excited state, and possible solvation effects highlights the need for more experimental and theoretical work to be done in order to more fully understand the *A*-band photodissociation of 1-bromo-2-iodoethane and other dihaloethanes. Additional experimental investigations such as magnetic circular dichroism (MCD), infrared emission, multiphoton ionization (MPI), femtosecond time-resolved pump–probe experiments[25,26,98–100] and others that have proven very useful in reaching a better understanding of the details of the *A*-band photodissociation dynamics of other iodoalkanes and dihaloalkanes are needed. These experiments and other relevant theoretical investigations should give a higher level of understanding of the interaction of the two C–X chromophores in the 1,2-dihaloethanes and how the initial photodissociation dynamics are correlated with the energy partitioning of the photofragments from the *A*-band photodissociation reaction.

ACKNOWLEDGMENTS

This work was supported by grants from the Research Grants Council (RGC) of Hong Kong, the Hung Hing Ying Physical Sciences Research Fund, the Committee on Research and Conference Grants (CRCG) from the University of Hong Kong, and the Large Items of Equipment Allocation 1993–94 from the University of Hong Kong.

[1] K. Kinmura and S. Nagakura, Spectrochim. Acta **17**, 166 (1961).
[2] A. Gedanken and M. D. Rowe, Chem. Phys. Lett. **34**, 39 (1975).
[3] A. Gedanken, Chem. Phys. Lett. **137**, 462 (1987).
[4] T. Donohue and J. Wiesenfeld, Chem. Phys. Lett. **33**, 176 (1975).
[5] T. Donohue and J. Wiesenfeld, J. Chem. Phys. **63**, 3130 (1975).
[6] W. H. Pence, S. L. Baughchum, and S. L. Leone, J. Phys. Chem. **85**, 3844 (1981).
[7] P. Brewer, P. Das, G. Ondrey, and R. Bersohn, J. Chem. Phys. **79**, 720 (1983).
[8] W. P. Hess, S. J. Kohler, H. K. Haugen, and S. R. Leone, J. Chem. Phys. **84**, 2143 (1986).
[9] R. Ogorzalek-Loo, G. E. Hall, H.-P. Haerri, and P. L. Houston, J. Phys. Chem. **92**, 5 (1987).
[10] F. G. Godwin, P. A. Gorry, P. M. Hughes, D. Raybone, T. M. Watkinson, and J. C. Whitehead, Chem. Phys. Lett. **135**, 163 (1987).
[11] Q. Zhu, J. R. Cao, Y. Wen, J. Zhang, Y. Huang, W. Fang, and X. Wu, Chem. Phys. Lett. **144**, 486 (1988).
[12] S. J. Riley and K. R. Wilson, Faraday Discuss. Chem. Soc. **53**, 132 (1972).
[13] R. K. Sparks, K. Shobatake, L. R. Carlson, and Y. T. Lee, J. Chem. Phys. **75**, 3838 (1981).
[14] G. N. A. Van Veen, T. Baller, A. E. Devries, and N. J. A. Van Veen, Chem. Phys. **87**, 405 (1984).
[15] M. D. Barry and P. A. Gorry, Mol. Phys. **52**, 461 (1984).
[16] C. Paterson, F. G. Godwin, and P. A. Gorry, Mol. Phys. **60**, 729 (1987).
[17] F. G. Godwin, C. Paterson, and P. A. Gorry, Mol. Phys. **61**, 827 (1987).
[18] J. F. Black and I. Powis, Chem. Phys. **125**, 375 (1988).
[19] I. Powis and J. F. Black, J. Phys. Chem. **93**, 2461 (1989).
[20] R. Ogorzalek-Loo, H.-P. Haerri, G. E. Hall, and P. L. Houston, J. Chem. Phys. **90**, 4222 (1989).
[21] D. W. Chandler, M. H. M. Janssen, S. Stolte, R. N. Strickland, J. W. Thoman, Jr., and D. H. Parker, J. Phys. Chem. **94**, 4839 (1990).
[22] N. E. Triggs, M. Zahedi, J. W. Nibler, P. A. Debarber, and J. J. Valentini, J. Chem. Phys. **96**, 2756 (1992).
[23] G. E. Hall, T. J. Sears, and J. M. Frye, J. Chem. Phys. **90**, 6234 (1989).

[24] J. W. G. Mastenbroek, C. A. Taatjes, K. Nauta, M. H. M. Janssen, and S. Stolte, J. Phys. Chem. **99**, 4360 (1995).
[25] J. L. Knee, L. R. Khundar, and A. H. Zewail, J. Chem. Phys. **83**, 1996 (1985).
[26] L. R. Khundar and A. H. Zewail, Chem. Phys. Lett. **142**, 426 (1987).
[27] D. G. Imre, J. L. Kinsey, A. Sinha, and J. Krenos, J. Phys. Chem. **88**, 3956 (1984).
[28] M. O. Hale, G. E. Galica, S. G. Glogover, and J. L. Kinsey, J. Phys. Chem. **90**, 4997 (1986).
[29] G. E. Galica, B. R. Johnson, J. L. Kinsey, and M. O. Hale, J. Phys. Chem. **95**, 7994 (1991).
[30] K. Q. Lao, M. D. Person, P. Xayaroboun, and L. J. Butler, J. Chem. Phys. **92**, 823 (1990).
[31] F. Markel and A. B. Myers, Chem. Phys. Lett. **167**, 175 (1990).
[32] A. B. Myers and F. Markel, Chem. Phys. **149**, 21 (1990).
[33] F. Markel and A. B. Myers, J. Chem. Phys. **98**, 21 (1993).
[34] P. G. Wang and L. D. Zeigler, J. Phys. Chem. **97**, 3139 (1993).
[35] B. R. Johnson and J. L. Kinsey, J. Phys. Chem. **100**, 18937 (1996).
[36] F. Duschek, M. Schmitt, P. Vogt, A. Materny, and W. Kiefer, J. Raman Spectrosc. **28**, 445 (1997).
[37] M. Shapiro and R. Bersohn, J. Chem. Phys. **73**, 3810 (1980).
[38] S. K. Gray and M. S. Child, Mol. Phys. **51**, 189 (1984).
[39] M. Shapiro, J. Phys. Chem. **90**, 3644 (1986).
[40] M. Tadjeddine, J. P. Flament, and C. Teichteil, Chem. Phys. **118**, 45 (1987).
[41] H. Guo and G. C. Schatz, J. Chem. Phys. **93**, 393 (1990).
[42] Y. Amatatsu, K. Morokuma, and S. Yabushita, J. Chem. Phys. **94**, 4858 (1991).
[43] H. Guo and G. C. Schatz, J. Phys. Chem. **95**, 3091 (1991).
[44] H. Guo, J. Chem. Phys. **96**, 2731 (1992).
[45] A. D. Hammerich, U. Manthe, R. Kosloff, H.-D. Meyer, and L. S. Cederbaum, J. Chem. Phys. **101**, 5623 (1994).
[46] Y. Amatatsu, S. Yabushita, and K. Morokuma, J. Chem. Phys. **104**, 9783 (1996).
[47] M. K. Dzvonik, S. Yang, and R. Bersohn, J. Chem. Phys. **61**, 4408 (1974).
[48] M. Kawasaki, S. J. Lee, and R. Bersohn, J. Chem. Phys. **63**, 809 (1975).
[49] P. M. Kroger, P. C. Demou, and S. J. Riley, J. Chem. Phys. **65**, 1823 (1976).
[50] T. K. Minton, P. Felder, R. J. Brudzynski, and Y. T. Lee, J. Chem. Phys. **81**, 1759 (1984).
[51] D. Krajnovitch, L. J. Butler, and Y. T. Lee, J. Chem. Phys. **81**, 3031 (1984).
[52] G. N. A. Van Veen, T. Baller, A. E. DeVries, and M. Shapiro, Chem. Phys. **93**, 277 (1985).
[53] Q.-X. Xu, K.-H. Jung, and R. B. Bernstein, J. Chem. Phys. **89**, 2099 (1988).
[54] W. K. Kang, K. W. Jung, D. C. Kim, K.-H. Jung, and H. S. Im, Chem. Phys. **196**, 363 (1995).
[55] W. K. Kang, K. W. Jung, D.-C. Kim, and K.-H. Jung, J. Chem. Phys. **104**, 5815 (1995).
[56] R. J. Donovan, F. G. M. Hathorn, and D. Husain, Trans. Faraday Soc. **64**, 3192 (1968).
[57] T. F. Hunter, S. Lunt, and K. S. Kristjansson, J. Chem. Soc., Faraday Trans. 2 **79**, 303 (1983).
[58] E. Gerck, J. Chem. Phys. **79**, 311 (1983).
[59] S. Uma and P. K. Das, Can. J. Chem. **72**, 865 (1994).
[60] D. H. Fairbrother, K. A. Briggman, E. Wietz, and P. C. Stair, J. Chem. Phys. **101**, 3787 (1994).
[61] P. L. Ross and M. V. Johnston, J. Phys. Chem. **99**, 4078 (1995).
[62] S. Uma and P. K. Das, Chem. Phys. Lett. **241**, 335 (1995).
[63] S. Uma and P. K. Das, J. Chem. Phys. **104**, 4470 (1996).
[64] J. Zhang and D. G. Imre, J. Chem. Phys. **89**, 309 (1988).
[65] D. L. Phillips, B. A. Lawrence, and J. J. Valentini, J. Phys. Chem. **95**, 7570 (1991).
[66] D. L. Phillips, B. A. Lawrence, and J. J. Valentini, J. Phys. Chem. **95**, 9085 (1991).
[67] D. L. Phillips and A. B. Myers, J. Chem. Phys. **95**, 226 (1991).
[68] D. L. Phillips, J. J. Valentini, and A. B. Myers, J. Phys. Chem. **96**, 2039 (1992).
[69] W. M. Kwok and D. L. Phillips, Chem. Phys. Lett. **235**, 260 (1995).
[70] D. L. Phillips and W. M. Kwok, Chem. Phys. Lett. **241**, 267 (1995).
[71] S. Q. Man, W. M. Kwok, and D. L. Phillips, J. Phys. Chem. **99**, 15705 (1995).
[72] W. M. Kwok and D. L. Phillips, J. Chem. Phys. **104**, 2529 (1996).
[73] W. M. Kwok and D. L. Phillips, J. Chem. Phys. **104**, 9816 (1996).
[74] S.-Q. Man, W. M. Kwok, A. E. Johnson, and D. L. Phillips, J. Chem. Phys. **105**, 5842 (1996).
[75] W. M. Kwok, P. K. Ng, G. Z. He, and D. L. Phillips, Mol. Phys. **90**, 127 (1997).
[76] D. L. Phillips and A. B. Myers, J. Raman Spectrosc. **28**, 839 (1997).
[77] X. Zheng and D. L. Phillips, Chem. Phys. Lett. **286**, 79 (1998).
[78] X. Zheng and D. L. Phillips, J. Chem. Phys. **108**, 5772 (1998).
[79] X. Zheng and D. L. Phillips, Chem. Phys. Lett. **292**, 295 (1998).
[80] A. B. Myers, B. Li, and X. Ci, J. Chem. Phys. **89**, 1876 (1988).
[81] M. O. Trulson and R. A. Mathies, J. Chem. Phys. **84**, 2068 (1986).
[82] B. Li and A. B. Myers, J. Phys. Chem. **94**, 4051 (1990).
[83] E. J. Heller, J. Chem. Phys. **62**, 1544 (1975).
[84] S. Y. Lee and E. J. Heller, J. Chem. Phys. **71**, 4777 (1979).
[85] E. J. Heller, R. L. Sundberg, and D. J. Tannor, J. Phys. Chem. **86**, 1822 (1982).
[86] A. B. Myers and R. A. Mathies, in *Biological Applications of Raman Spectroscopy*, edited by T. G. Spiro (Wiley, New York, 1987), Vol. 2, p. 1.
[87] A. B. Myers, in *Laser Techniques in Chemistry*, edited by A. B. Myers and T. R. Rizzo (Wiley, New York, 1995), p. 325.
[88] For vibrational assignments, see X. Zheng and D. L. Phillips, Vib. Spectrosc. **17**, 73 (1998).
[89] For normal coordinate calculations see AIP document No. PAPS JCPSA6-110-015903 for 7 pages of tables of the Cartesian coordinates, complete force fields, calculated vibrational frequencies and normal-mode coefficients. Order by PAPS number and journal reference from American Institute of Physics, Physics Auxiliary Publication Service, 500 Sunnyside Boulevard, Woodbury, New York 11797-2999. Fax: 516-576-2223, e-mail: paps@aip.org. The price is $1.50 for each microfiche (98) pages or $5.00 for photocopies of up to 30 pages, and $0.15 for each additional page over 30 pages. Airmail additional. Make checks payable to the American Institute of Physics.
[90] B. U. Curry, Ph.D. dissertation, University of California, Berkeley, 1983.
[91] T. K. Minton, G. M. Nathanson, and Y. T. Lee, J. Chem. Phys. **86**, 1991 (1984).
[92] P. B. Roussel, P. B. Lightfoot, F. Caralp, V. Catoire, R. Lesclaux, and W. Forst, J. Chem. Soc., Faraday Trans. **87**, 2367 (1991).
[93] E. Villenave and R. Lesclaux, Chem. Phys. Lett. **236**, 376 (1995).
[94] G. M. Nathanson, T. K. Minton, S. F. Shane, and Y. T. Lee, J. Chem. Phys. **90**, 6157 (1990).
[95] B. H. Lengsfield, P. E. M. Siegbahn, and J. Liu, J. Chem. Phys. **81**, 710 (1984).
[96] J. Pacansky, W. Koch, and M. D. Miller, J. Am. Chem. Soc. **113**, 317 (1991).
[97] W. M. Kwok and D. L. Phillips, Mol. Phys. **90**, 315 (1997).
[98] L. R. Khundkar and A. H. Zewail, J. Chem. Phys. **92**, 231 (1990).
[99] B. J. Schwartz, J. C. King, J. Z. Zhang, and C. B. Harris, Chem. Phys. Lett. **203**, 503 (1993).
[100] K. Saitow, Y. Naitoh, K. Tominaga, and Y. Yoshihara, Chem. Phys. Lett. **262**, 621 (1996).